Science Robotics
AAAS

robotics.sciencemag.org/cgi/content/full/6/50/eabd5476/DC1

Supplementary Materials for

Microrobotic laser steering for minimally invasive surgery

Peter A. York*, Rut Peña, Daniel Kent, Robert J. Wood

*Corresponding author. Email: pyork@g.harvard.edu

Published 13 January 2021, *Sci. Robot.* **6**, eabd5476 (2021)
DOI: 10.1126/scirobotics.abd5476

The PDF file includes:

Other Supplementary Material for this manuscript includes the following:

(available at robotics.sciencemag.org/cgi/content/full/6/50/eabd5476/DC1)

Supplementary Materials

Additional considerations for miniaturization

There are several additional considerations for miniaturization that should be taken into account when integrating this device with a specific surgical laser. In particular, there are tradeoffs between device length, width, stand-off distance, and laser spot size. These can be seen with the assistance of Fig. S4, which schematically represents the collimation and focusing of the fiber-delivered beam. Assuming the use of ideal thin lenses and small angles of refraction, the product of the image size and ray angle is invariant, and terms involving $\sin(\theta)$ can be replaced by θ. Under these assumptions, there is the following simple relation for spot size radius y_4 as a function of collimator focal length f_c, focusing lens focal length f_f, and fiber core radius y_1:

$$y_4 = \frac{f_f}{f_c} y_1$$

Assuming there is some desired stand-off distance from the device to the surgical site, we see that there is an inverse relationship between spot size and collimator focal length. This means that the device length must be increased in order to reduce the size of the laser spot. For example, if a stand-off distance of 20 mm is desired and one is using a fiber with a 500 μm core, which is typical of flexible CO2 laser fibers, such as the Lumenis FiberLase (Lumenis Ltd., Yokneam, Israel), a 10 mm collimator length would be needed to achieve a 1 mm spot size. Thus, achieving a larger stand-off distance and smaller spot size will have an adverse effect on miniaturization, requiring elongation of the device.

Conversely, the scaling of the device diameter is largely a function of the angle of dispersion of the laser as it exits the fiber, i.e., the fiber's numerical aperture. This follows from the scaling of the radius of the collimated beam y_2, which can be written as a function of the collimator focal length f_c and the angle of dispersion of the fiber θ_1:

$$y_2 = f_c \theta_1$$

For a given collimator focal length, collimated beam size scales directly with the fiber's angle of dispersion. Increasing the size of the collimated beam requires the use of larger optical components, which necessitates increasing device diameter. This is especially important when scaling the galvanometer components; based on the analysis in the Design section, we expect that device diameter will scale roughly linearly with collimated beam diameter for a given desired range of motion. This means that if small device diameter is desired, a fiber with suitably low angle of dispersion should be used. For example, if a 1 mm collimated beam diameter is desired, as we assumed in the Design section, with a collimator focal length of 10 mm, a fiber with a dispersion angle of 0.1 rad would be needed. For this scenario, an optical cable such as the PIR 400/500 (Arts Photonics GmbH, Berlin, Germany) with core diameter 400 μm and numerical aperture 0.1 rad could be used.

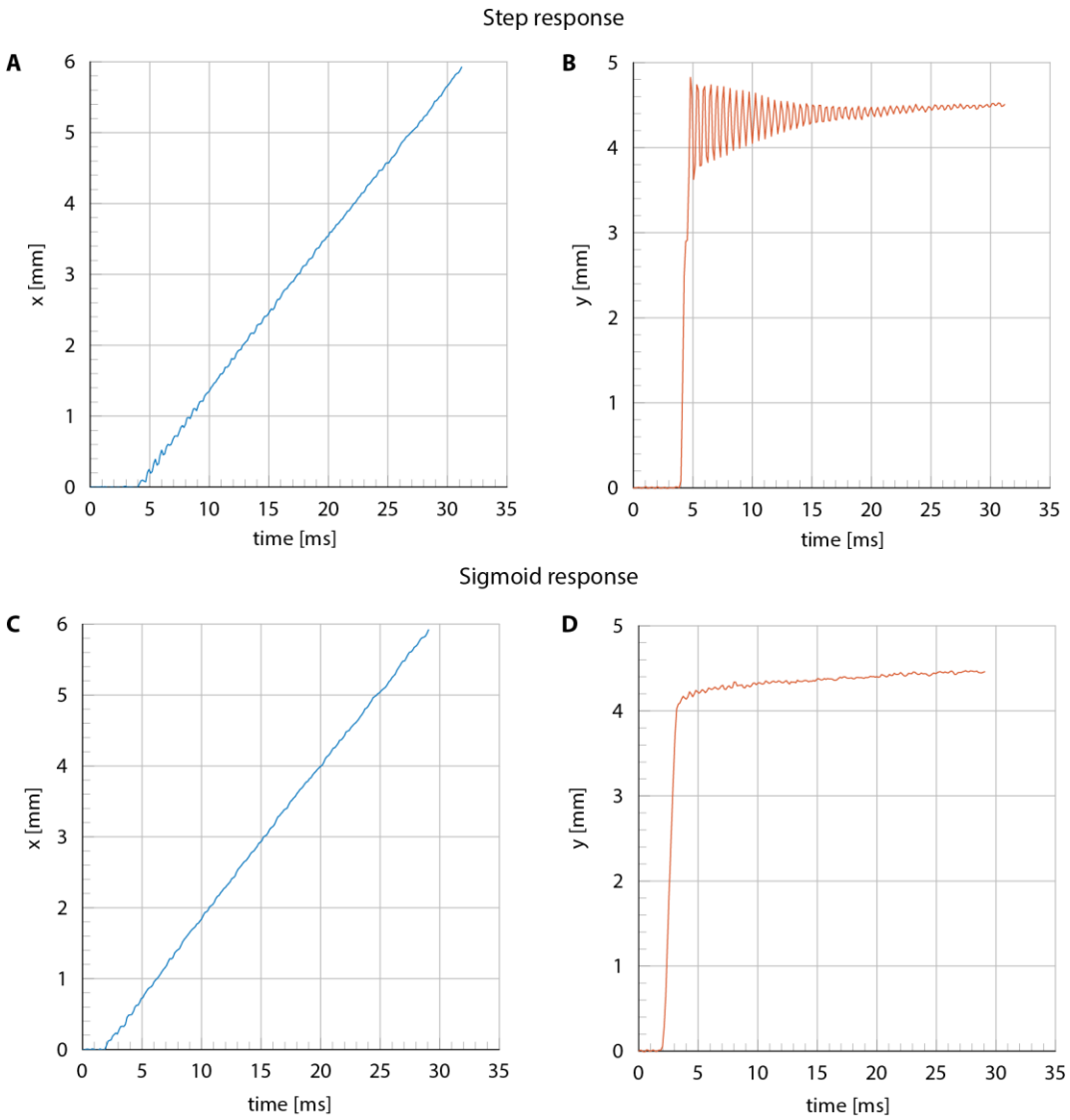

Fig. S1. Time history of step and sigmoid responses. Raw data from Movie S4 showing the laser position of a step response (**A-B**) compared to a sigmoid (**C-D**) response. The sigmoid input ensures that the motion profile has finite jerk, which prevents the oscillations that can be seen in the step response. The tradeoff is some loss in absolute speed (i.e., rise time): the maximum y component of laser velocity is 5900 mm/s for the step input and 3900 mm/s for the sigmoid input.

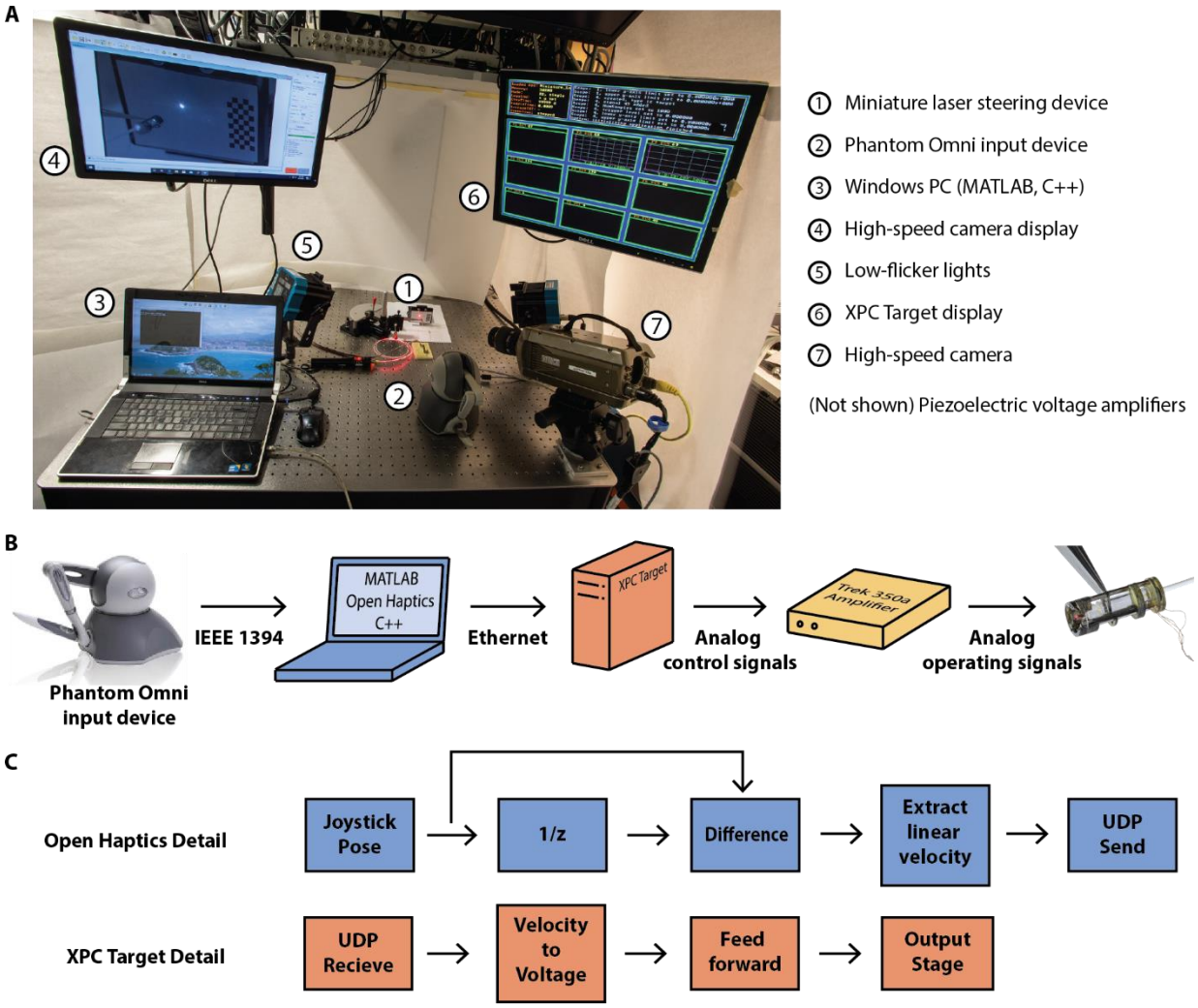

Fig. S2. Experimental setup and system architecture. A Measurement setup for collecting laser spot position with high-speed camera, low-flicker lighting, and supporting equipment. **B** Hardware architecture and signal flow for laser teleoperation from the joystick input device to the laser steering tool. **C** Program flow for mapping joystick pose to actuator inputs within the Open Haptics API and XPC Target.

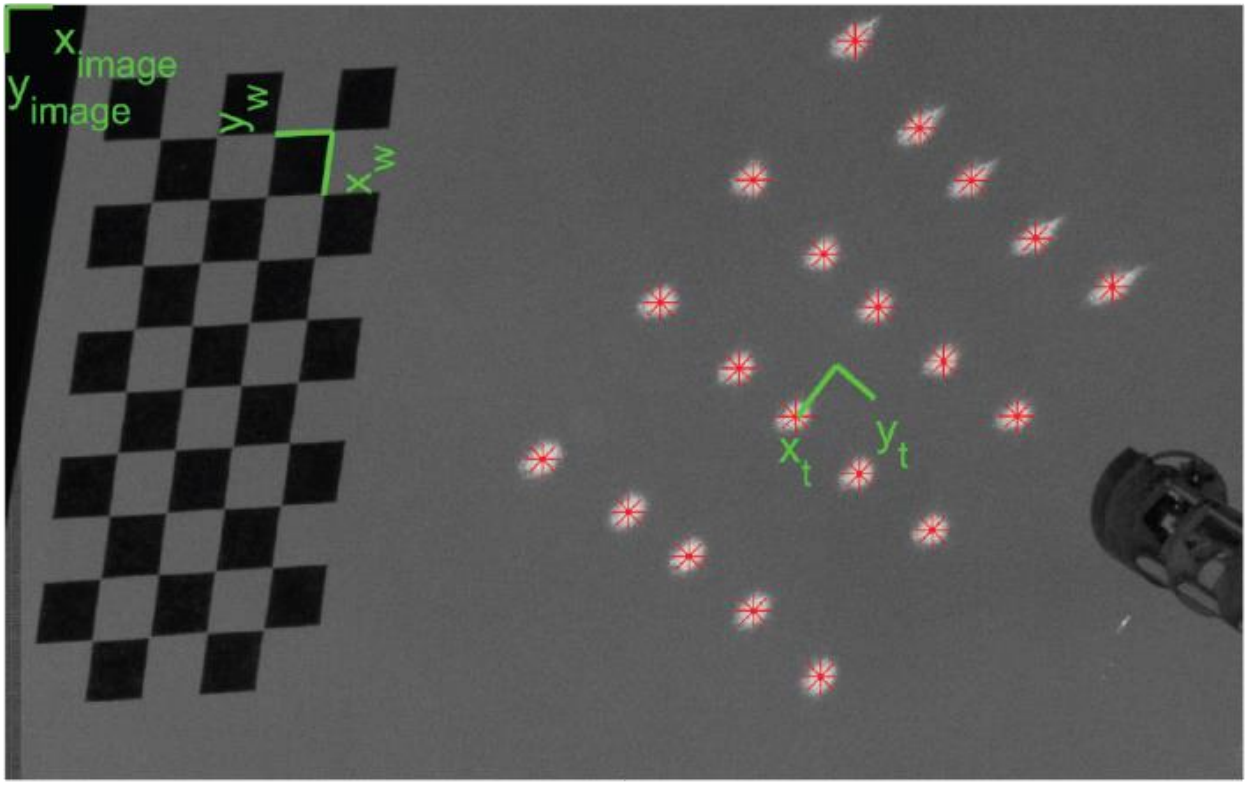

Fig. S3. Measurement of laser position repeatability. This image contains 20 sampled points in the laser workspace superimposed onto a single image. The data for 10 such trials is compiled and shown in Fig. 5A.

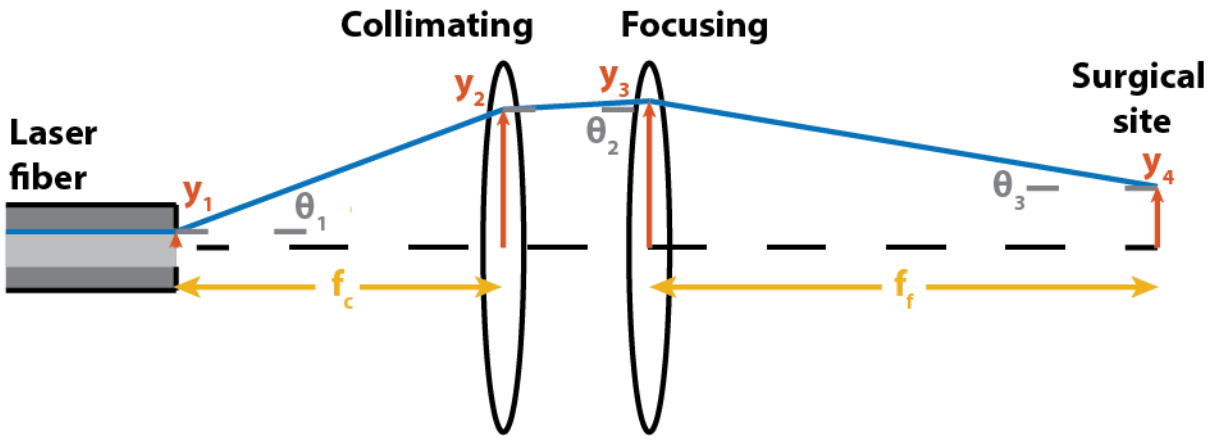

Fig. S4. Optical component schematic. The nominal laser beam size throughout the device is a function of the laser fiber's core size y_1, dispersion angle θ_1 and the focal lengths f_c and f_f of the collimating and focusing optics.

Movie S1. Principle of operation. Individual components are highlighted and their contribution to overall device function described. The relationship between input control voltage and output laser position is shown.

Movie S2. Device assembly. Assembly is straightforward due to the modular design and fabrication approach. This video shows zoomed-in detail of the entire assembly process.

Movie S3. Hysteresis compensation. Setpoint regulation with and without hysteresis compensation, which dramatically improves the quality of control.

Movie S4. Sigmoid profiling of control inputs. Using sigmoid input profiles avoids exciting the resonant modes of the mirrors, which is important for high-speed control. The time history of the trajectories is shown in Fig. S1.

Movie S5. High-speed trajectory following. The same star trajectory is traced at low (7.8 mm/s) and high speeds (3900 mm/s). Both the rendered images and the zoomed-in motion of the device are shown.

Movie S6. Complex trajectory following. Using high-speed control the device draws two complex images: a logo of the laser steering tool and the Harvard Microrobotics Lab logo.

Movie S7. Multimodal control. By leveraging the high bandwidth of the device, high-speed trajectories can be interposed on low-speed ones to allow on-the-fly control over the area of laser application.

Movie S8. Colonoscope integration and deployment. The laser steering device is integrated with a commercial colonoscope (Olympus CF-100L); teleoperated and automated operation are shown.